Author(s): Sonin, E. B. & Torizuka, K. & Kyynäräinen, J. M. & Pekola, Jukka & Tvalashvili, G. K.

Title: Wave acoustics for propagation of ultrasound along a vortex array in superfluid 3He-A

Year: 1992

Version: Final published version

Please cite the original version:

Sonin, E. B. & Torizuka, K. & Kyynäräinen, J. M. & Pekola, Jukka & Tvalashvili, G. K. 1992. Wave acoustics for propagation of ultrasound along a vortex array in superfluid 3He-A. Physical Review B. Volume 45, Issue 18. 10536-10543. ISSN 1098-0121 (printed). DOI: 10.1103/physrevb.45.10536.

Wave acoustics for propagation of ultrasound along a vortex array in superfluid ^{3}He-A

E. B. Sonin,* K. Torizuka, J. M. Kyynäräinen, and J. P. Pekola
Low Temperature Laboratory, Helsinki University of Technology, 02150 Espoo, Finland

G. K. Tvalashvili
Institute of Physics of the Georgian Academy of Sciences, 380077 Tbilisi, Georgia
(Received 29 April 1991; revised manuscript received 29 January 1992)

A wave-acoustics theory has been developed to describe the propagation of zero sound parallel to vortex lines in rotating ^{3}He-A. We show that a diffraction "shadow" is formed in which the wave amplitude is suppressed by interference around vortices. This phenomenon contributes to the experimentally observed effect of rotation on the sound amplitude and exceeds the attenuation at large core radii. The dependence of the diffraction contribution on the angular velocity changes drastically at the transition from vortices with a finite core to coreless vortices when the magnetic field is decreased to zero. We derive conditions for the applicability of the effective-medium theory and the classical geometrical acoustic method in describing sound propagation along vortices.

I. INTRODUCTION

Ultrasonics is helpful for studying order-parameter collective modes[1] in the superfluid phases of ^{3}He and structures of vortices in the rotating superfluid.[2] For interpretation of experiments, an effective-medium approach,[3] with parameters of the fluid averaged over the periodical vortex array or, alternatively, a geometrical acoustics method[2] have been used. Our paper develops an acoustic wave theory for interpretation of ultrasonic experiments in rotating ^{3}He-A.[4] We consider the phenomenon of sound wave diffraction around vortex cores, and explain the observed drastic change in the character of ultrasound propagation along vortices when the magnetic field is decreased to zero. Our theory provides another length scale (diffraction length d) for sound propagation, which is important when it is larger than the size of the vortex core.

A remarkable property of ^{3}He-A is the possibility of *coreless* vortices[5] in which $\nabla\times\mathbf{v}_s$ is not confined to a core of definite size, unlike in ^{4}He II or in ^{3}He-B. In contrast to vortices with a hard (coherence length $\xi_0\simeq 10^{-6}$ cm) or a soft (magnetic length $\xi_H \geq 10^{-3}$ cm) core, there is, in this case, no length scale besides the size of the vortex cell (vortex lattice constant $b\simeq 10^{-2}$ cm). This structure may exist only in very low magnetic fields: $H \ll H_d$, where $H_d \simeq 3$ mT is the dipolar field. Especially such a vortex can expand over the whole vessel in the limit $H\rightarrow 0$. In a rotating fluid, when the vortex density is fixed by the solid-body rotation condition, each coreless vortex occupies the whole cell in the vortex array. In the wave-acoustic theory presented here, we discuss diffraction of sound by vortices with and without a core, and show that ultrasound is a suitable probe to detect the coreless vortex. In fact, we have experimentally observed the continuous crossover between the two types of vortices in low magnetic fields.

II. EXPERIMENT

Our experimental setup has been described in detail elsewhere.[2] The sound cell consists of two X-cut quartz crystals, $L=4$ mm apart, and the cylindrical volume between them has a diameter of 6 mm. Pulses of ultrasound at odd harmonic frequencies of 8.9 MHz, 12 μsec long, were transmitted parallel to the magnetic field $\mathbf{H}$ and the axis of rotation $\mathbf{\Omega}$. The propagation of ultrasound along $\mathbf{H}$ in liquid at rest provides a convenient reference level for the received signal in a rotating fluid. When $H \gg H_d$, $\hat{\boldsymbol{l}}$ is normal to $\mathbf{H}$ everywhere in the cell. Any deviation from this "planar" texture contributes to the sound signal, and thus provides a probe for studies of the vortex structure.

Figure 1 depicts the dependence of the received sound amplitude on the angular velocity Ω in various magnetic fields and for two frequencies, $f=26.8$ and 44.7 MHz. Our procedure to obtain the data was as follows: Initially, a magnetic field $H_0 \gg H_d$ was applied to determine the amplitude $A_\perp \propto \exp(-\alpha_\perp L)$. The field was then swept from H_0 to the value H of Fig. 1. Next the ^{3}He sample was accelerated to the desired Ω and the sound amplitude $A(\Omega)$ in the equilibrium rotation state was recorded. Figure 1 shows the relative change $-\Delta A/A_\perp \equiv -[A(\Omega)-A_\perp]/A_\perp$, which is a function of Ω and H. We use amplitude $A(\Omega)$ rather than attenuation $\alpha(\Omega)$ in the analysis of the data, since in general the signal A, directly calculated in our theory and measured in an experiment, cannot be presented by just one attenuation parameter α in the form $\exp(-\alpha L)$.

The main feature of Fig. 1 is the smooth evolution of the Ω dependence of $-\Delta A/A_\perp$ with decreasing field. When $H > H_d$, $-\Delta A/A_\perp$ increases linearly with Ω at small Ω, whereas when $H \simeq 0$, $-\Delta A/A_\perp$ has a nonzero value at all Ω, and depends only weakly on Ω. This indicates evolution of the $\hat{\boldsymbol{l}}$ texture: in large fields, the varia-

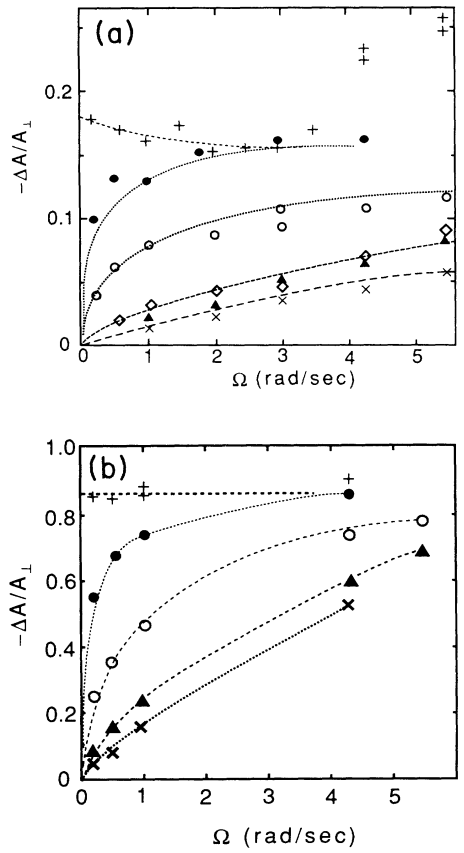

FIG. 1. Magnitude of the measured relative change in the amplitude of ultrasound ($-\Delta A/A_\perp$) vs the angular velocity (Ω) at $p=29.3$ bars with two different frequencies: (a) $f=26.8$ MHz at the relative temperature $T/T_c=0.9$ and (b) $f=44.7$ MHz at $T/T_c=0.85$. The symbols correspond to different magnetic fields employed: (a) (×), $H=4.0$ mT; (△), 1.6 mT; (◇), 1.2 mT; (○), 0.8 mT; (●), 0.5 mT; and (+), $H=0$; (b) (×), $H=3.4$ mT; (△), 2.2 mT; (○), 1.4 mT; (●), 0.7 mT; and (+), $H=0$. The lines through different sets of data points were used to obtain values of the extrapolated slopes $(-\Delta A/A_\perp)/\Omega$ in Fig. 4. Most of the data in (a) are from Kyynäräinen *et al.* (Ref. 2, Fig. 12).

tion of $\hat{l}$ around each vortex takes place in an area much smaller than the unit cell in the vortex array, whereas in zero magnetic field nonsingular vorticity spans the whole unit cell even at the lowest Ω. Especially at $\Omega\rightarrow 0$, a Mermin-Ho (MH) texture[6] occupies the whole experimental chamber.

III. SIMPLE APPROACHES: EFFECTIVE MEDIUM AND GEOMETRICAL ACOUSTICS

In anisotropic ^{3}He-A, sound attenuation α and velocity c can be written as [7]

$$\alpha=\alpha_\parallel\cos^4(\theta)+2\alpha_c\cos^2(\theta)\sin^2(\theta)+\alpha_\perp\sin^4(\theta) \quad (1)$$

and

$$c=c_{0F}-\Delta c_\parallel\cos^4(\theta)-2\Delta c_c\cos^2(\theta)\sin^2(\theta) -\Delta c_\perp\sin^4(\theta) , \quad (2)$$

where θ is the angle between the orbital vector $\hat{l}$ and the sound wave vector $\mathbf{k}$. α and c/c_{0F} are shown in Figs. 2(a) and 2(b), respectively, as functions of θ, where c_{0F} is the zero sound velocity in the normal Fermi-liquid phase. The MH texture corresponds to $\theta=0$ at the center and $\theta=\pi/2$ at the perimeter of the chamber. In rotating ^{3}He the sound velocity $c(\mathbf{r})$ and attenuation $\alpha(\mathbf{r})$ are periodic functions of the position $\mathbf{r}$, since the direction of $\hat{l}$ varies periodically on the xy plane.

In the effective-medium approach the wave propagating along the rotation axis (the z axis) is assumed to be a plane wave over the whole sound cell. Then the relative change of the signal is given by

$$-\frac{\Delta A}{A_\perp}=1-\exp(-\tilde{\alpha}L) , \quad (3)$$

where the attenuation parameter $\tilde{\alpha}$ taking into account the effect of vortices is calculated by averaging the attenuation α over the unit cell of the vortex lattice:

$$\tilde{\alpha}=\int_S[\alpha(r)-\alpha_\perp]dS . \quad (4)$$

The factor $\exp(-\alpha_\perp L)$ determines attenuation of the plane wave in the perpendicular $\hat{l}$ texture as well and it cancels out when we derive the expression for the relative signal $-\Delta A/A_\perp$. At a low rotation velocity ($r_c \ll b$),

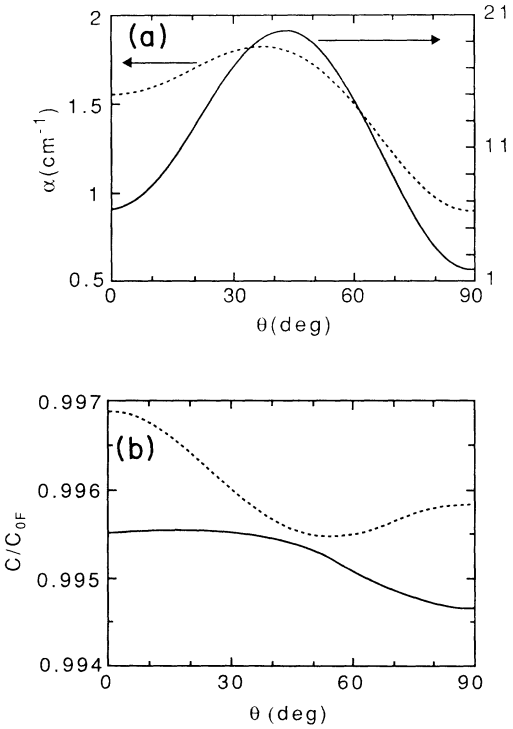

FIG. 2. (a) Attenuation and (b) relative velocity of zero sound. Dashed and solid lines correspond to $f=26.8$ MHz and $T/T_c=0.9$, and to $f=44.7$ MHz and $T/T_c=0.85$, respectively. The values of attenuation and the velocity parameters were computed by Wojtanowski (Ref. 10). Here θ is the angle between the sound-wave vector $\mathbf{k}$ and the orbital vector $\hat{l}$ in the vortex texture. In (a) the scale at left is for 26.8 MHz and at right for 44.7 MHz; $p=29.3$ bars for both cases.

$\tilde{\alpha} \approx \Delta\alpha (r_c/b)^2$, where $\Delta\alpha$ is the difference of the attenuation inside and outside of the core, r_c is the core radius, and b is the lattice constant which is of the order of the intervortex distance. At a high rotation velocity when the vortex core occupies most of the unit cell ($b \sim r_c$) $\tilde{\alpha}$ is of order $\Delta\alpha$. However, one cannot expect that such a simple approach is always valid since deviations of the wave front from a plane develop when sound propagates from the transmitter to the receiver.

In order to include the effect of deviation from a plane wave, the geometrical acoustics methods were used in the preliminary analysis of our ultrasonic experiments.[2] In such a picture the phenomenon of diffraction manifests itself as interference of different rays at points in the receiver plane. The rays have been determined from the wave equation for the sound pressure p (attenuation is neglected):

$$\frac{\partial^2 p(\mathbf{r},z,t)}{\partial t^2} - \nabla\cdot[c^2(\mathbf{r})\nabla p(\mathbf{r},z,t)] = 0 \ . \tag{5}$$

To determine the regime where this method is valid, one may impose the standard condition $d\lambda/dr \ll 1$: the wavelength λ must not vary considerably over a distance of order λ. However, an important feature of our geometry is that the wavelength which satisfies this condition is determined, not by the wave-number component k_z along the rotation axis, but by the wave number $q = \sqrt{\omega^2/c(\mathbf{r})^2 - k_z}$ on the xy plane. Therefore, the requirement for the validity of geometrical acoustics is $|dq/dr| \ll q^2$. This is because the parameters of the medium vary only across the xy plane. For the rays emitted normally to the transmitter plane $k_z = \omega/c(\mathbf{r}_0)$ and

$$|q| \simeq \left[\frac{\Delta c}{c_0} k_0\right]^{1/2} , \quad \left|\frac{dq}{dr}\right| \simeq \frac{\Delta c}{c_0}\frac{1}{q}\frac{k_0^2}{r_c} \ . \tag{6}$$

Here $\mathbf{r}_0$ is the position vector on the transmitter plane where the ray is emitted, $k_0 = \omega/c_0$ is the magnitude of the wave vector of the plane wave propagating in the fluid at rest with sound velocity c_0, and $\Delta c(\mathbf{r}) = c(\mathbf{r}) - c_0$. Since q is of the order of the inverse of the diffraction length d which is $\sim\sqrt{L/k_0}$, as will be discussed in Sec. V, one may use the quasiclassical theory if

$$\frac{r_c^2}{k_0 L^3} \gg \left[\frac{\Delta c}{c_0}\right]^2 . \tag{7}$$

But the procedure employed in Ref. 2 did not take into account all classical rays coming to a point on the receiver plane, but only the extremal ones which were emitted normally by the transmitter plane. In fact, trajectories from the area of the transmitter plane within a scale $\simeq (|dq/dr|)^{-1/2}$ contribute to the signal at a point on the receiver. It is possible to restrict oneself to the extremal trajectories when this scale is smaller than the scale r_c over which the medium parameters vary considerably. This gives the inequality

$$\left[\frac{\Delta c}{c_0}\right]^2 \gg \frac{1}{r_c^2 k^3 L} \ . \tag{8}$$

One cannot satisfy both conditions, Eqs. (7) and (8), unless the core radius r_c exceeds the diffraction length d. All shortcomings of the aforementioned simple approaches have prompted us to undertake a more general analysis of the problem as presented below.

IV. WAVE ACOUSTICS IN VORTEX ARRAYS

When a wave is propagating along the rotation axis (the z axis), it is natural to look for a solution of the wave equation as a sum over the Bloch functions in the center of the Brillouin zone of the vortex lattice. We thus write for the sound pressure p at frequency $f = \omega/2\pi$

$$p(\mathbf{r},z,t) = \exp(-i\omega t)\sum_n A_n f_n(\mathbf{r})\exp(iK_n z) \ . \tag{9}$$

After substitution of Eq. (9) into the wave equation, Eq. (5), one sees that the functions $f_n(\mathbf{r})$, periodic on the xy plane, are solutions of equations

$$-\nabla^2 f_n(\mathbf{r}) - \frac{2}{c(\mathbf{r})}\nabla[\Delta c(\mathbf{r})]\cdot\nabla f_n(\mathbf{r}) + \left[k_0^2 - \frac{\omega^2}{c(\mathbf{r})^2}\right] f_n(\mathbf{r}) = q_n^2 f_n(\mathbf{r}) \ . \tag{10}$$

Here ∇ is spatial gradient on the xy-plane, $q_n^2 = k_0^2 - K_n^2$. The eigenvalues q_n are determined by periodic boundary conditions for the unit cell of the vortex lattice. The periodic perturbation in Eq. (10) is due to the two last terms on the left-hand side. However, the first of them will be neglected here since its effect is proportional to the parameter $(\Delta c/c_0)(1/q_n r_c)$, which is small for cases under consideration. Equation (10) is then similar to the equation of a quantum particle in the field produced by the space variation of the sound velocity, viz.,

$$-\nabla^2 f_n(\mathbf{r}) + U(\mathbf{r}) f_n(\mathbf{r}) = q_n^2 f_n(\mathbf{r}) \ . \tag{11}$$

The "potential"

$$U(\mathbf{r}) = 2k_0^2\frac{\Delta c(\mathbf{r})}{c_0} \tag{12}$$

is smallest when the sound velocity is at its minimum.

The solution of Eq. (11) for a wave propagating over a chamber of length L is obtained as follows: The transmitter at $z=0$ sends a plane wave, which means, assuming unit strength for the emitted wave, that the amplitudes A_n of harmonics are the coefficients of the expansion for unity. If $f_n(\mathbf{r})$ are orthonormalized, then

$$1 = \sum_n A_n f_n(\mathbf{r}) \tag{13}$$

and

$$A_n = \int_S f_n^*(\mathbf{r})\, dS \ . \tag{14}$$

Here integration is carried over the area S of the unit vortex cell. The receiver at $z=L$ detects a signal averaged over this plane. The averaged pressure $\bar{p}$ at the receiver [the ratio of the averaged pressure to the pressure $\exp(ik_0 L - i\omega t)$ of the plane wave in the fluid at rest] is

$$\bar{p}=\sum_n A_n \exp[i(K_n-k_0)L]\frac{1}{S}\int_s f_n(\mathbf{r})dS$$
$$=\sum_n p_n \exp[i(K_n-k_0)L]\ , \tag{15}$$

where the weight of the nth harmonic

$$p_n=|A_n|^2/S \tag{16}$$

is introduced. The experimental quantity $-\Delta A/A_\perp$ is to be compared with $1-|\bar{p}|$.

V. WAVE ACOUSTICS FOR VORTICES WITH A CORE

We shall further approximate the real cell of the nonaxisymmetric vortex array by the axisymmetric Wigner-Seitz cell of radius b (called the lattice constant earlier and hereafter), determined by Ω:

$$\Omega=\frac{\kappa}{2S}=\frac{\kappa}{2\pi b^2}\ . \tag{17}$$

Here $\kappa=\nu h/2m_3$ is the circulation per unit cell, where ν is the number of circulation quanta, and m_3 is the mass of a ^{3}He atom. Only axisymmetric harmonics should be taken into account, and n is a radial "quantum number." For vortices with a core it is assumed that the variation of the sound velocity is restricted to the core region, whose radius is considered as r_c. A steplike simple model may be used: $c(r)=c_0$ for $r\le r_c$, and $c(r)=c_0+\Delta c$ for $r>r_c$ where Δc is a constant. The harmonics are then given by the zeroth-order Bessel functions:

$$f_n(r)\propto\begin{cases}D_n J_0(q'_n r) & \text{for } r\le r_c\\ J_0(q_n r)+B_n Y_0(q_n r) & \text{for } r>r_c\ .\end{cases} \tag{18}$$

Here $q'^2_n=q_n^2-U=q_n^2-2(\Delta c/c_0)k_0^2$. The factors D_n and B_n are determined from the conditions of continuity of $f_n(r)$ and $f'_n(r)$ at $r=r_c$. Using expansions of Bessel functions at small arguments $q'_n r_c$ and $q_n r_c$ one obtains

$$B_n=\frac{\pi U r_c^2}{2[2-q'^2_n r_c^2\ln(1/q_n r_c)]}\ ,$$
$$D_n=\frac{2-q_n^2 r_c^2\ln(1/q_n r_c)}{2-q'^2_n r_c^2\ln(1/q_n r_c)}\ . \tag{19}$$

The eigenvalues q_n can be determined from the condition $f'_n(b)=0$ at the boundary of the Wigner-Seitz cell, imitating the periodic boundary condition for the real vortex lattice. For the basic harmonic, i.e., for the first term in the sum, the eigenvalue is

$$q_0=\begin{cases}(1/b)\sqrt{[2/\ln(b/r_c)]} & \text{for } \ln(b/r_c)\gg 2/Ur_c^2\\ (r_c/b)\sqrt{U} & \text{for } \ln(b/r_c)\ll 2/Ur_c^2\ .\end{cases} \tag{20}$$

We then find that $p_0\simeq 1$. Together with the sum rule $\sum_n p_n=1$, this means that the total weight of the higher harmonics is rather small and, therefore, that the energy of the sound wave is carried mostly by the basic harmonic. However, keeping only $n=0$ in the sum causes no effect other than some variation in the phase of the received signal, the amplitude remaining the same as for the fluid at rest. But the signals from different harmonics arrive at the receiver with different phases, and the interference between them may result in a variation ΔA of the signal amplitude. In order to find the weight of the harmonics for $n>0$ in the sum, Eq. (15), the asymptotic expressions of the Bessel functions at large arguments qb were used to calculate A_n. We thus obtain

$$p_n=\frac{\pi U^2 r_c^4}{2q_n^3 b^3}\frac{[2-q_n^2 r_c^2\ln(1/q_n r_c)]^2}{[2-q'^2_n r_c^2\ln(1/q_n r_c)]^2+(\pi U r_c^2)^2}\ . \tag{21}$$

For small Ω (large b) the amplitude variation is proportional to Ω and is determined by the amplitudes of higher harmonics. The sum of these contributions is well estimated by the integral over $q_n\simeq\pi n/b$:

$$-\Delta A/A_\perp=1-|\bar{p}|$$
$$\simeq 1-\mathrm{Re}(\bar{p}) \tag{22}$$
$$=\frac{b}{\pi}\int_0^\infty dq\, p(q)[1-\cos(q^2L/2k_0)].$$

Equation (22) introduces a new spatial scale which is crucial for the present analysis: the diffraction length $d=\sqrt{L/k_0}$. The wave numbers $q\sim 1/d$ are relevant for the integral in Eq. (22). The effect of the core depends on the ratio between d and another spatial scale

$$l_U=r_c\exp\left[\frac{2}{Ur_c^2}\right]=r_c\exp\left[\frac{1}{k_0^2 r_c^2}\frac{c_0}{\Delta c}\right] \tag{23}$$

characterizing the potential inside of the core. If $d\gg l_U$, the sound wave does not penetrate into the core and the approximate formula for the signal variation is

$$-\Delta A/A_\perp=\frac{2}{b^2}\int_0^\infty dq\frac{[1-\cos(q^2L/2k_0)]}{q^3(\ln q r_c)^2}$$
$$\simeq\frac{\pi L}{b^2 k_0[\ln(L/2k_0 r_c^2)]^2}\ . \tag{24}$$

The impenetrable-core model is valid both for repulsive ($\Delta c>0$) and for attractive ($\Delta c<0$) potentials in the core. In the latter case, l_U is the characteristic linear dimension of the localized state which corresponds to the lowest harmonic, but its contribution is not important compared to that of continuum states when the impenetrable-core model is valid. In the opposite limit of a weak core potential, when $q\simeq\sqrt{k_0/L}$ exceeds $1/l_U$, the contribution of rotation to the signal amplitude is

$$-\Delta A/A_\perp=\frac{U^2 r_c^4}{2b^2}\int_0^\infty dq\frac{1}{q^3}[1-\cos(q^2L/2k_0)]$$
$$=\frac{\pi}{4b^2}Lk_0^3 r_c^4\left[\frac{\Delta c}{c_0}\right]^2\ . \tag{25}$$

In the limit $b\to\infty$ ($\Omega\to 0$), according to the integral approximation for the sum of Eq. (15), the signal $-\Delta A/A_\perp$ is linearly increasing as a function of Ω.

TABLE I. Important length scales. $H_d \simeq 3$ mT.

Length scale	Symbol	Value
Sound path length	L	0.4 cm
Sound wavelength	λ	$\sim 2\times 10^{-4}$ cm
Diffraction length	$d=\sqrt{L/k_0}$	$\sim 10^{-2}$ cm
Vortex-lattice constant	$b=\sqrt{\kappa/2\pi\Omega}$	$\sim 10^{-2}/\sqrt{\Omega}$ cm (Ω in units of rad/s)
Dipolar length	ξ_d	$\sim 10^{-3}$ cm (29 bars)
Magnetic length	$\xi_H=\xi_d H_d/H$	$\sim 2.5\times 10^{-3}/H$ cm (29 bars, H in units of mT)
Radius of a vortex core	$r_c=\max(\xi_d,\xi_H)$	

The calculated decrease of amplitude was obtained without including attenuation terms in the wave equation, and it results only from interference of a large number of harmonics at the receiver. This phenomenon may be considered as diffraction of the sound wave by the cylindrical vortex core.

A more detailed analysis of the signal distribution over the receiver at $z=L$ shows that a shadow, or a diffraction region with a characteristic linear dimension $d=\sqrt{L/k_0}\sim 10^{-2}$ cm arises around the core, where the signal is suppressed, down to zero for the impenetrable core. It is natural to expect that the signal variation will be proportional to Ω as long as the diffraction regions of vortices do not overlap, i.e., when $b \gg d$. At small $b \leq d$, the distance between eigenvalues, $q_{n+1}-q_n \simeq \pi/b$ becomes larger than a typical $q \simeq d^{-1}$ determining the diffraction effect, causing the integral approximation of the sum to become poor. In the limit $b \ll d$, the whole sum is reduced to the first term and diffraction disappears. It is thus expected that at $b \leq d$ the amplitude variation $-\Delta A/A_\perp$ vs Ω deviates from a straight line with a constant slope and drops to zero after a few oscillations. One should remember, however, that we have discussed the variation of the signal due to diffraction only, having neglected attenuation in the bulk liquid. In the case of pure diffraction, the energy carried by the sound wave is not lost in the bulk, but is distributed among numerous interfering harmonics leading to nonvanishing $-\Delta A/A_\perp$.

Concluding this section, we refer to Table I where important length scales are given. It shows that diffraction on vortices is relevant for ultrasound experiments on ^{3}He-A vortices.

VI. ATTENUATION IN WAVE ACOUSTICS

In the wave-acoustic theory presented here sound attenuation in the bulk liquid may be included by introducing the factor $\exp(-\alpha_n L)$ for each harmonic in the sum of Eq. (15) where

$$\alpha_n = \int_S [\alpha(r)-\alpha_\perp]|f_n(\mathbf{r})|^2 dS \tag{26}$$

takes into account the effect of vortices. The most important term is α_0 since the weight of the basic harmonic considerably exceeds the weights of the higher components. When the potential inside the core is weak ($d \ll l_U$), the basic harmonic f_0 is nearly constant over the xy plane and the attenuation parameter α_0 coincides with the attenuation parameter $\tilde{\alpha}=\Delta\alpha r_c^2/b^2$ of the effective-medium theory[3] (see Sec. II). On the other hand, if the core potential is strong ($d \gg l_U$), the sound wave inside is strongly suppressed (it is repelled from the core), attenuation in the core affects the signal only marginally, and its effect vanishes altogether in the limit of the impenetrable core ($l_U \to 0$). The basic harmonic attenuation

$$\alpha_0=\Delta\alpha\frac{r_c^2}{b^2}\left[\frac{4}{U(0)r_c^2\ln(b/r_c)}\right]$$

$$=\Delta\alpha\frac{r_c^2}{b^2}\left[\frac{2}{k_0^2 r_c^2\ln(b/r_c)}\frac{c_0}{\Delta c}\right]\propto\frac{\Omega}{\ln\Omega} \tag{27}$$

then differs from the result of the effective-medium theory by the factor in the large parentheses which becomes small for the strong core potential. This suppression occurs as long as b exceeds l_U.

Attenuation is taken into account assuming that it does not influence the form of the harmonics f_n essentially. We expect α to be weak if its contribution to the sound wave spectrum,

$$\omega^2 \simeq c^2(k^2-2ik\,\Delta\alpha)\,, \tag{28}$$

is small, i.e., if $\Delta\alpha \ll k \simeq k_0$. However, in our geometry the wave propagates normally to the plane at which the parameters of the liquid vary. Therefore, a stronger condition is necessary to neglect the attenuation when solving the two-dimensional wave equation on the xy plane for the harmonics f_n: the attenuation contribution, proportional to $\Delta\alpha k_0$, must be small compared to the potential U. Together with Eq. (12) this gives an inequality

$$\Delta\alpha \ll (\Delta c/c_0)k_0\,. \tag{29}$$

If this condition is not valid one should include the attenuation terms when solving the equations for harmonics. But then one must deal with a problem of the wave equation with a complex-valued potential.

In Fig. 3 the dependence of the signal on the angular velocity Ω is shown for different attenuation parameters. The curves have been calculated numerically on the basis of the simplified core-structure model given above, but the other approximations of the solutions were not made. The analytical expressions for the strong potential [Eq. (24)] or for the weak potential [Eq. (25)] are not accurate enough for the parameters of the core to correspond to the experimental curve at $f=26.8$ MHz and $H=0.5$ mT in Fig. 1. The attenuation parameter was varied from

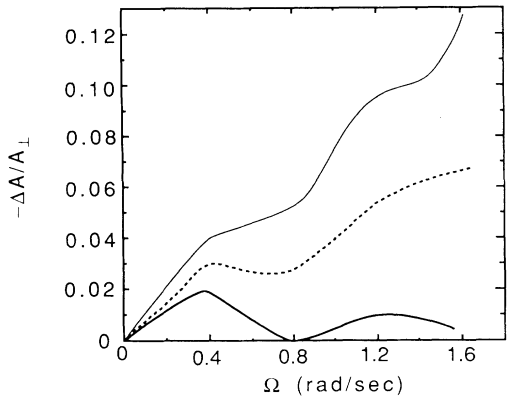

FIG. 3. Dependence of $-\Delta A/A_\perp$ on Ω, computed in the acoustic-wave theory for the core radius $r_c=50$ μm and for the experimental conditions of Fig. 1(a), with $H=0.5$ mT. The thick solid line is the pure diffraction contribution neglecting attenuation. The dashed and thin solid lines represent the total value of $-\Delta A/A_\perp$ when attenuation inside the vortex core is increased by $\Delta\alpha=0.5$ cm^{-1} and by $\Delta\alpha=1$ cm^{-1}, respectively. The latter case should best correspond to the experimental data at $H=0.5$ mT. Parameters employed in the calculation were $\Delta c/c_0\simeq 10^{-3}$ and $\nu=1$.

zero up to $\Delta\alpha=1$ cm^{-1}, corresponding to the data in Fig. 2. At zero attenuation two diffraction maxima are seen on the calculated curve up to $\Omega\simeq 1.6$ rad/sec. Attenuation removes the second maximum and makes the first much weaker, although the diffraction contribution to the slope of the $-\Delta A/A_\perp$ vs Ω curve remains considerable, in comparison with the attenuation effect. The curves in Fig. 3 were not calculated to higher angular velocities since the model is valid only if the core radius r_c is smaller than b.

VII. COMPARISON BETWEEN EXPERIMENTAL RESULTS AND WAVE-ACOUSTIC THEORY OF CORE VORTICES

The strong dependence of the diffraction signal on the core radius [the r_c^4 law, see Eq. (23)] makes a direct comparison with the experimental signal difficult: any inaccuracy, inevitable when determining r_c is strongly amplified. Therefore, primarily we prefer to compare the power laws. As a second step, when the power law has been found, we compare quantitatively the values of r_c from the theory of vortices with soft cores[8] with the values of r_c providing the best fit to the experiment.

In order to check how strong the effect of diffraction is on the linear slope of the curve $-\Delta A/A_\perp$ vs Ω at small Ω, the values of the slopes for the curves of Fig. 1 were plotted as a function of $1/H$ on a log-log scale in Fig. 4. It is expected that the core radius r_c does not differ substantially from the magnetic length $\xi_H=\xi_d H_d/H$,[8] if r_c exceeds the dipole length $\xi_d\simeq 10^{-3}$ cm. Such values of r_c show that the experiment is better described in the case of a weak core potential and, according to Eq. (25), the slope due to diffraction should be proportional to $r_c^4\propto\xi_H^4\propto 1/H^4$. On the other hand, the attenuation contribution to the slope, which may be determined in the case of a weak core potential from the effective-medium theory, is expected to be proportional to $r_c^2\propto\xi_H^2\propto 1/H^2$. It is seen from Fig. 4 that the experimental curve for $f=26.8$ MHz [data from Fig. 1(a)] and for not too strong magnetic fields corresponds to the $1/H^4$ law rather well. However, the curve for $f=44.7$ MHz [data from Fig. 1 (b)], with the variation of attenuation at the xy plane about ten times stronger, lies between the $1/H^4$ and $1/H^2$ laws, corresponding to the diffraction slope and the effective-medium slope, respectively. It should be mentioned that the condition of Eq. (29) is violated because of strong attenuation when $f=44.7$ MHz. Thus the effect of diffraction can be clearly revealed only at $f=26.8$ MHz [Fig. 1(a)].

Using the experimental values of the slope at $f=26.8$ MHz and the theoretical expression of Eq. (25), one can find the core radius by a fit to the experimental data. This gives values of r_c, not much different from the magnetic length ξ_H ($1.4\xi_H\le r_c\le 1.8\xi_H$), which confirms that the diffraction contribution to the experimental slope is strong, despite the fact that a maximum in the $-\Delta A/A_\perp$ vs Ω curves was not observed experimentally. In stronger magnetic fields, when $H\ge H_d$, we expect that $r_c\simeq\xi_d$ and that the slope should become independent of H. This explains the deviation from the $1/H^4$ law at strong fields ($H\ge 2$ mT$\sim H_d$), but the range of the experimental magnetic fields is not sufficient to follow perfectly such a crossover.

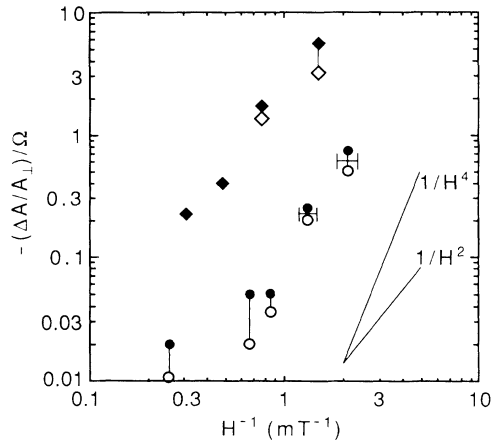

FIG. 4. Initial slopes $(-\Delta A/A_\perp)/\Omega$ of the experimental curves in Fig. 1, plotted as functions of $1/H$ on a log-log scale at $f=26.8$ MHz (lower set of points) and at $f=44.7$ MHz (upper set). The horizontal error bars correspond to the experimental inaccuracy in the value of H, which is negligible except at the lowest fields employed. The vertical error bars show the difference between the values of the slopes, obtained from the experimental points in Fig. 1 at the smallest Ω (◇,○) and from the extrapolation of smooth curves to $\Omega=0$, drawn through many experimental points (◇,●) in Fig. 1. The diffraction slope ($\propto 1/H^4$) and the effective-medium attenuation slope ($\propto 1/H^2$) are shown for comparison; the location of these lines in the figure is arbitrary.

VIII. CORELESS VORTICES

Let us consider the propagation of sound waves along coreless vortices. One of their distinctive features is that there is no other characteristic length scale except b. When b increases the space distribution of $c(r)$ transforms conformly. The sound wave has a tendency to localize inside the region with minimum velocity, and we consider the case when the velocity is smallest on a cylindrical surface of radius r_m around the axis of the Wigner-Seitz cell, i.e.,

$$\Delta c(r)=\Delta c_0(r-r_m)^2/2(\Delta r)^2 \ . \tag{30}$$

The parameter Δc_0 shows the scale of the sound velocity variation within a vortex cell and Δr describes the width of the annular potential well for the sound wave. We assume that r_m and Δr are on the order of b and increase linearly with it. We shall see later that for a large b the sound wave is localized at the bottom of the potential. This justifies the use of a parabolic form for the well, and Eq. (11) gives harmonics similar to eigenfunctions of the linear quantum oscillator:

$$\begin{aligned} &q_n=\sqrt{2n+1}/l \ , \\ &f_n \propto H_n\left[\frac{r-r_m}{l}\right]\exp\left[-\frac{(r-r_m)^2}{l^2}\right] . \end{aligned} \tag{31}$$

Here $H_n(x)$ are the Hermite polynomials of nth order and the length

$$l=\left[\frac{\Delta r}{k_0}\left[\frac{c_0}{\Delta c_0}\right]^{1/2}\right]^{1/2} \tag{32}$$

determines the linear dimension of the ground state which is proportional to $\sqrt{b}$ and is, therefore, small compared to b at large lattice constants. The weight of the different harmonics at the bottom of the well is (only even harmonics $n=2m$ contribute to the sum)

$$p_{2m}=\frac{\sqrt{\pi}(2m)!}{2^{2(m-1)}(m!)^2}\frac{r_m l}{b^2}\sim\frac{4}{\sqrt{m}}\frac{r_m l}{b^2} \quad \text{as } m\to\infty \ , \tag{33}$$

and by replacing the sum in Eq. (15) by an integral one obtains the relative amplitude of the received signal

$$\begin{aligned} |\bar{p}| &= \frac{4r_m l^2}{b^2}\int_0^\infty dq \exp(-q^2L/2k_0) \\ &= \frac{4\sqrt{2\pi}r_m l^2}{b^2}\left[\frac{k_0}{L}\right]^{1/2} \\ &= \frac{4\sqrt{2\pi}r_m \Delta r}{b^2}\left[\frac{1}{k_0 L}\frac{c_0}{\Delta c_0}\right]^{1/2} . \end{aligned} \tag{34}$$

Since $r_m \sim \Delta r \propto b$, the signal amplitude does not depend on b (i.e., on Ω). A distinctive feature of the propagation of ultrasound along coreless vortices is that at $\Omega>0$ (even in the limit $\Omega\to 0$) the signal differs from that at $\Omega=0$. When rotation is started, the signal amplitude jumps to a new value during formation of a periodic vortex array with a large number of vortices.

The relevant harmonics contributing to the integral in Eq. (34) correspond to large quantum numbers $n\simeq q^2l^2\propto b$, and may be described quasiclassically using the geometrical-acoustic theory. The linear dimension of the region they occupy is on the order of $l\sqrt{n}\simeq ql^2$, and it should be smaller than Δr, which is of order b. The latter condition assures that all relevant harmonics are localized within the well. Using Eq. (32) for l and bearing in mind that $\Delta r\simeq b$ and that the relevant q's are inversely proportional to d, this condition leads to the inequality

$$k_0 L\,\Delta c_0/c_0 \gg 1 \ . \tag{35}$$

Approximating the sum by an integral is valid until typical values of $q\simeq d^{-1}$, contributing to the integral, exceed the distance $\sim 1/(ql^2)\simeq\sqrt{k_0 L(c_0/\Delta c_0)}/\Delta r$ between eigenvalues of the wave vectors in the potential well. This imposes the inequality

$$b\sim\Delta r \gg L\sqrt{\Delta c_0/c_0} \ . \tag{36}$$

At smaller $b\ll L\sqrt{\Delta c_0/c_0}$, the sum is approaching the value of the first term related to the ground state in the potential well, since other terms vanish owing to the fast variation of their phases:

$$|\bar{p}|\to p_0=\frac{4\sqrt{\pi}r_m l}{b^2}=\frac{4\sqrt{\pi}r_m}{b^2}\left[\frac{\Delta r}{k_0}\left[\frac{c_0}{\Delta c_0}\right]^{1/2}\right]^{1/2} . \tag{37}$$

In contrast to Eq. (34), this result cannot be obtained from the quasiclassical theory since it refers to the ground state of the harmonic oscillator, which is poorly described by quasiclassics. Deriving Eq. (37), we assumed that the ground-state size l is smaller than the intervortex distance b. This is valid if

$$b\gg\frac{1}{k_0}\left[\frac{c_0}{\Delta c_0}\right]^{1/2} . \tag{38}$$

At larger Ω when this condition is violated, the sound approaches a plane wave and the wave-acoustics effects should vanish.

Therefore, in the case $k_0 L\Delta c_0/c_0\gg 1$, our analysis presents the following picture. At small Ω ($b\gg L\sqrt{\Delta c_0/c_0}$), the wave is localized in a narrow region around points with minimum sound velocity (guidance effect). Because of the interference between tightly lying harmonics, the signal at the receiver for the rotating liquid is strongly suppressed, in comparison to the signal from fluid at rest, and is on the order of the small parameter $\sqrt{c_0/\Delta c_0}/\sqrt{k_0 L}$ ($-\Delta A/A_\perp$ is about unity). When Ω increases in the interval $L\sqrt{\Delta c_0/c_0}\gg b\gg(1/k_0)\sqrt{c_0/\Delta c_0}$, the basic harmonic contribution is mostly registered by the receiver, the phase of higher harmonics varying fast even between neighboring harmonics. The signal $|\bar{p}|$ is on the order of $[(c_0/\Delta c_0)^{1/2}/k_0 b]^{1/2}$, according to Eq. (37), and increases ($-\Delta A/A_\perp$ decreases) in proportion to $\sqrt{\Omega}$.

With further increase of Ω [$b \ll (1/k_0)\sqrt{c_0/\Delta c_0}$], the interference suppression effects disappear and $|\bar{p}|$ approaches unity. In this region the most important signal is due to the bulk attenuation, which may be determined using the effective-medium theory since the form of the wave is weakly modulated. This gives an Ω independent signal.

Comparing with the experiment, we should take into account that the relevant inequalities of our theory [Eq. (35) above all] are not satisfied very well. The presented scenario assumes also that the potential well for ultrasound has a shape of the valley on the cylindrical surface of radius r_m. The deviation from cylindrical symmetry breaks this valley into a set of minima along vertical lines around the center of each cell in the vortex array. Then our scenario only gives an averaged qualitative picture. The deviations are more important for the MH structure,[6] since the surface of minima is close to the boundary of the unit vortex cell.

It is worth pointing out that the effective-medium theory, ignoring the wave guidance effects, predicts an Ω-independent signal for straight vortices (see, however, discussion on attenuation for vortex loops in Ref. 9). The guidance is expected to decrease the attenuation suppression of the signal if the attenuation is weaker in the region of smaller sound velocity, as was the case in our experiment. This means that the attenuation-governed signal suppression, $-\Delta A/A_\perp$, increases with Ω, unlike in the case of interference suppression. On the other hand, in accordance with the latter scenario, the signal $-\Delta A/A_\perp$ for zero magnetic field in Fig. 1(a) decreases while Ω increases up to $\Omega \simeq 3$ rad/sec, where a phase transition in the $\hat{l}$ texture is suggested.[9] But parameters of the coreless vortex in our experiment are not favorable for quantitative comparison. The quantity $k_0 L\, \Delta c_0/c_0$, assumed to be large in our analysis, is only 1.6 but, nevertheless, the region where a decrease in $-\Delta A/A_\perp$ is expected lies around $\Omega = 1$ rad/sec, as in our experiment.

IX. SUMMARY

A wave-acoustics theory has been developed for ultrasound propagating along vortices in rotating superfluid ^{3}He. Within this framework, conditions have been derived for the validity of the effective-medium theory and the geometrical-acoustics methods, which were used in earlier analyses of zero-sound propagation in a vortex array. It is shown experimentally that the diffraction phenomenon, which was not considered in those theories, contributes significantly to the magnitude of the effect of vortices on the ultrasound signal when the diffraction length is on the order of or larger than the core radius. A simple analytical model has been suggested to describe the effect of diffraction on propagation of ultrasound along coreless vortices.

The theory, as presented, still has a number of shortcomings, which can be overcome by more sophisticated models: (i) The theoretical investigations[8] imply that the vortices in ^{3}He-A are nonaxisymmetric, unlike those in our simplified discussion. The real vortex unit cell is also nonaxisymmetric. This weakness in the theory can be removed by including nonaxisymmetric harmonics into sound-wave expansions. (ii) A more realistic shape, instead of a steplike variation, can be introduced for the velocity profile around the vortex. (iii) In the experiment attenuation is rather strong sometimes, and the effect of α on the shape of the harmonic eigenfunctions should be taken into account as well.

ACKNOWLEDGMENTS

We thank G. A. Kharadze, O. V. Lounasmaa, and G. E. Volovik for stimulating discussions, A. J. Manninen for contributions to the experiment, and W. Wojtanowski for providing us with a computer program to calculate attenuation and velocity parameters in ^{3}He-A. E.B.S. and G.K.T. thank the Low Temperature Laboratory of the Helsinki University of Technology for hospitality.

*Permanent address: A. F. Ioffe Physico-Technical Institute, St. Petersburg, 194021, Russia.

[1] W. P. Halperin and E. Varoquaux, in *Helium Three,* edited by W. P. Halperin and L. P. Pitaevskii (Elsevier, Amsterdam, 1990), Chap. 7.

[2] J. M. Kyynäräinen, J. P. Pekola, K. Torizuka, A. J. Manninen, and A. V. Babkin, J. Low Temp. Phys. **82**, 325 (1991); J. P. Pekola, K. Torizuka, A. J. Manninen, J. M. Kyynäräinen, and G. E. Volovik, Phys. Rev. Lett. **65**, 3293 (1990); **67**, 1055 (E) (1991).

[3] A. L. Fetter, J. A. Sauls, and D. L. Stein, Phys. Rev. B **28**, 5061 (1983); M. Nakahara, T. Ohmi, T. Tsuneto, and T. Fujita, Prog. Theor. Phys. Jpn. **62**, 874 (1979).

[4] Wave acoustics in textures of stationary ^{3}He-A_1 were discussed by P. G. de Vegvar, R. Movshovich, E. L. Ziercher, and D. M. Lee, Phys. Rev. Lett. **57**, 1028 (1986); see also P. G. de Vegvar, Ph.D. thesis, Cornell University, 1986 (unpublished).

[5] P. W. Anderson and G. Toulouse, Phys. Rev. Lett. **38**, 508 (1977); T.-L. Ho, Phys. Rev. B **18**, 1144 (1978).

[6] N. D. Mermin and T.-L. Ho, Phys. Rev. Lett. **36**, 594 (1976); **36**, 832(E) (1976).

[7] J. W. Serene, Ph.D. thesis, Cornell University, 1974 (unpublished); P. Wölfle, in *Progress in Low Temperature Physics,* edited by D. F. Brewer (North-Holland, Amsterdam, 1978), Vol. 7A, Chap. 3; P. Wölfle and V. E. Koch, J. Low Temp. Phys. **30**, 61 (1978).

[8] M. M. Salomaa and G. E. Volovik, Rev. Mod. Phys. **59**, 533 (1987); **60**, 573(E) (1988).

[9] K. Torizuka, J. P. Pekola, A. J. Manninen, and G. E. Volovik, Pis'ma Zh. Eksp. Teor. Fiz. **53**, 263 (1991).

[10] W. Wojtanowski (private communication).